GEOPHYSICAL RESEARCH LETTERS, VOL. 21, NO. 8, PAGES 713-716, APRIL 15, 1994

Estimation of oceanic hydrothermal heat flux from heat flow and depths of midocean ridge seismicity and magma chambers

Aristeo M. Pelayo and Seth Stein
Department of Geological Sciences, Northwestern University, Evanston, Illinois

Carol A. Stein
Department of Geological Sciences, University of Illinois at Chicago

Abstract. The difference between the heat flow predicted by thermal models of the lithosphere and that measured at the seafloor can be used to estimate the cooling by hydrothermal circulation. However, this approach may yield an overestimate because measurements in thinly sedimented young crust are typically made at topographic lows where hydrothermal circulation may systematically lower heat flow. To circumvent this bias we estimate the cooling using the depths of midocean ridge earthquakes and magma chambers in addition to heat flow data. The results indicate deeper hydrothermal circulation at slow spreading ridges, and higher near-axial hydrothermal heat loss at fast spreading ridges. The predicted global hydrothermal heat flux is ~80% of that for models constrained only by heat flow.

Introduction

Estimating the volume and age distribution of the heat and water transported by hydrothermal circulation through oceanic crust is important in understanding the evolution of the oceanic crust, and its effect on the chemistry of the oceans and atmosphere [*Rona et al.*, 1983]. Because water flow is measured directly only at isolated sites, indirect methods are used to estimate the net global hydrothermal flux. The difference between the heat flow predicted by thermal models and the lower values observed for lithosphere <50-70 Ma can be used to estimate the heat transported by hydrothermal flow [e.g., *Sleep and Wolery*, 1978] as ~11×10^{12} W, ~1/3 of the net oceanic heat flux [*Stein and Stein*, 1994]. Most is transported not by high-temperature water flow near the ridge, but by lower-temperature flow in older lithosphere.

A potential difficulty with such estimates is a possible sampling bias in heat flow measurements, which require ~10 m of sediment. Most suitable sites in young lithosphere are in sediment-filled lows between bare rock outcrops. The measurements [*Langseth et al.*, 1992] accord with models [*Lowell*, 1980] indicating that in thinly sedimented regions, water should descend at low points and upwell at highs, giving lower heat flow at lows. Unless unusually thick sediments cover almost all basement topography [*Davis et al.*, 1989], heat flow measurements are biased toward lower values [*Becker and Von Herzen*, 1983] and resulting hydrothermal heat flux estimates are upper bounds.

Paper number 94GL00395
0094-8534/94/94GL-00395$03.00

Here, we estimate the hydrothermal heat flux using constraints from off-ridge heat flow data and the depths of near-ridge seismicity and magma chambers, both of which occur deeper than expected without hydrothermal cooling [*Morton and Sleep*, 1985; *Lin and Parmentier*, 1989; *Phipps Morgan and Chen*, 1993] This estimate does not depend on the near-ridge heat flow and thus should minimize bias due to sampling.

Thermal Model and Constraints

We use a thermal model for the lithosphere (Figure 1) including heat sources reflecting latent heat released when material cools below the solidus, and heat sinks representing cooling by hydrothermal circulation [*Morton and Sleep*, 1985]. Sources are distributed at and off the ridge about the 1185°C isotherm, down to the assumed crustal base at 5 km. Heat sinks extend out to 50 Ma, the approximate age beyond which the predicted cumulative hydrothermal heat flux is essentially constant, suggesting that water flow no longer transfers significant amounts of heat at the seafloor [*Stein and Stein*, 1994]. The plate thickness, basal temperature, and thermal conductivity are from the GDH1 model [*Stein and Stein*, 1992], such that if no hydrothermal cooling occurred the heat flow away from the ridge would be that for GDH1. Other parameters are from *Morton and Sleep* [1985]. Because the model gives temperatures as a function of distance rather than age, we can examine how hydrothermal heat flux depends on spreading rate.

The near-ridge constraints are the variations with spreading rate of the depths of seismically-imaged axial magma chamber tops [*Purdy et al.*, 1992] and large ($M \geq 5$) midocean ridge earthquakes [*Huang and Solomon*, 1988]. We assume that the magma chamber top coincides with the 1185°C isotherm [*Morton and Sleep*, 1985] and that earthquakes occur above the 750°C isotherm, as observed for comparable sized oceanic intraplate earthquakes [*Wiens and Stein*, 1983]. Because of location uncertainty, we treat the earthquakes as within 5 km of the axis. Ridge microearthquakes, with moments less about 10^{13} N-m, which occur deeper than the centroids of the teleseismically recorded events [*Toomey et al.*, 1988], were not used given the lack of knowledge about off-ridge microearthquake depths. The off-ridge constraint is the observed heat flow for >10 Ma [*Stein and Stein*, 1994].

After trying many combinations, we chose 2 simple heat sink distributions, $s(t)$, (Table 1). Both have sinks concentrated within 0.1 Ma of the axis, and the same net sinks integrated out to 50 Ma, 9×10^{13} J m^{-2}. In model I, sinks extend to 4 km depth at the axis, and 2 km off axis. In model II, sinks extend to 2 km and 1 km respectively. We compute thermal structures for half-spreading rates of 2.5 to 80 mm/yr, keeping the sink

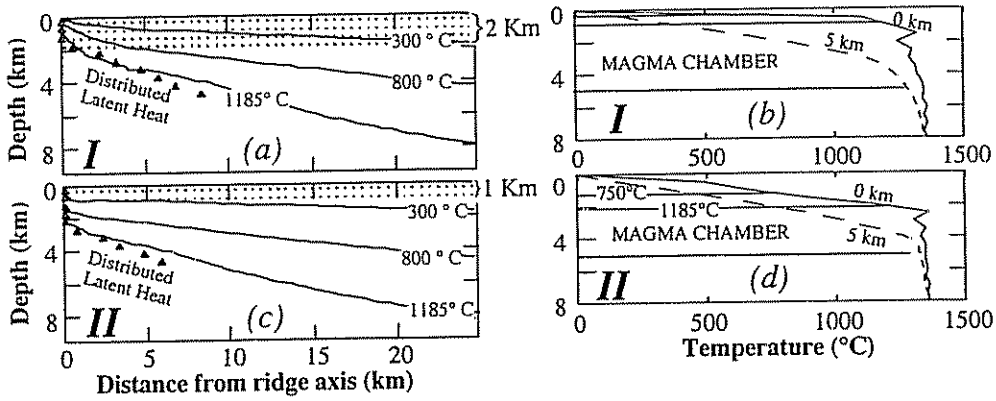

Fig. 1. Comparison of thermal models for two hydrothermal sink distributions at 40 mm/yr half-spreading rate. Models I and II have different sink distributions (stipple), both at and off the ridge axis, and hence different geotherms beneath the axis (0 km) and 5 km away. Depths to the predicted 750°C and 1185°C isotherms, corresponding to the predicted deepest seismicity and magma chamber tops, are shown for the ridge axis geotherms. Geotherm oscillations are artifacts of the 0.5-km computation grid.

distribution with age the same, so the sink density in space is $s(t)$ divided by the half rate [*Morton and Sleep*, 1985].

The observed seismicity and magma chambers deepen for slower rates (Figure 2), presumably because slower ridges are cooler and thus stronger to greater depth. The models predict different near-ridge temperatures. For a given spreading rate, model II is cooler and predicts a deeper magma chamber and seismicity. Models with no hydrothermal cooling (labeled "0") predict maximum earthquake depths and magma chambers shallower than observed.

Model I is more consistent with earthquake and magma chamber depths at slow ridges. Model II better fits magma chamber depths at fast ridges. For rates ≥25 mm/yr, model I predicts temperatures >1185°C at the magma chamber depths, because the shallow sinks provide insufficient cooling. On the other hand, model II can be precluded for rates <15-20 mm/yr because the ridge axis would freeze, as the heat lost by cooling exceeds that supplied.

Given the uncertainties in the data and the model's simplicity, the agreement is satisfactory if not ideal. The different models for the fast and slow spreading ridges imply that near-ridge hydrothermal cooling depends on more than age. Model I, with the deeper sinks and better fit for slow ridges, is consistent with *Purdy et al.*'s [1992] suggestion that water penetrates deeper for slow spreading because faults extend deeper.

The mean heat flow with age (Figure 3a) is systematically lower than predicted by GDH1. The larger standard deviations at young ages presumably reflect spatial variations in hydrothermal circulation due to local topography, sediment cover, and permeability which can be studied with site-specific models [*Fisher et al.*, 1990]. We use only the mean heat flow because our interest is in the overall hydrothermal heat loss versus age.

Although near the ridge the earthquake and magma chamber depths provide constraints on the depth of cooling, away from the ridges heat flow data for ages >10 Ma (Figure 3a) constrain only the temperature gradient. Hence, models I and II are "composite" models. For simplicity, they have the same net hydrothermal loss for ages >0.05 Ma, and thus the same net loss to 50 Ma. We thus treat the two models as one for ages ≥5 Ma where the heat flow predictions are essentially the same. For younger ages the effect of spreading rate is noticeable, so curves for half rates 2.5 and >10 mm/yr are shown. For the slower rate, heat sources are restricted to the axis, and the near-ridge sinks make the predicted heat flow just off-axis less than further away. This artifact of the model parameterization occurs for very slow spreading and has no significance.

The composite model predicts heat flow within a few Ma of the axis higher than the mean observed. We believe that this

Table 1. Vertically integrated heat sink distribution $s(t)$

Age (Ma)	Model I (W m^{-2})	Model II (W m^{-2})
0	2.8	12.8
$0 < t \le 0.01$	1.4	6.4
$0.01 < t \le 0.05$	1.4	$0.2\ t^{-1/2}$
$0.05 < t \le 50$	$0.2\ t^{-1/2}$	$0.2\ t^{-1/2}$
$t > 50$	0	0

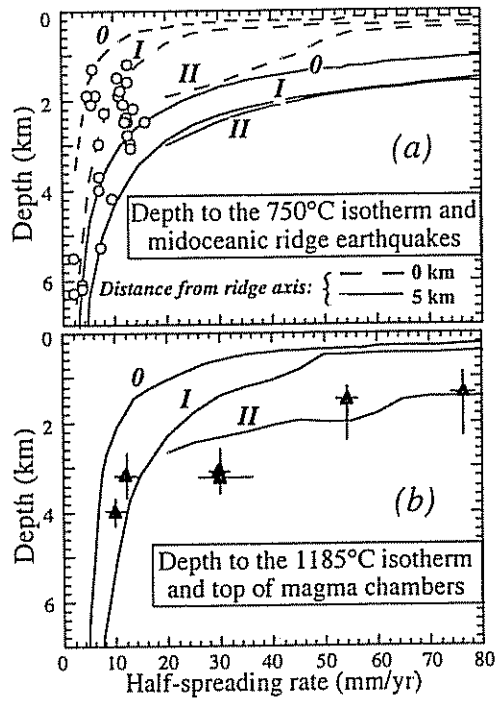

Fig. 2. *a*: Midocean ridge earthquake depths and predicted 750°C isotherm at distances of 0 and 5 km from ridge axis. *b*: Depths to magma chambers and predicted 1185°C isotherm below ridge.

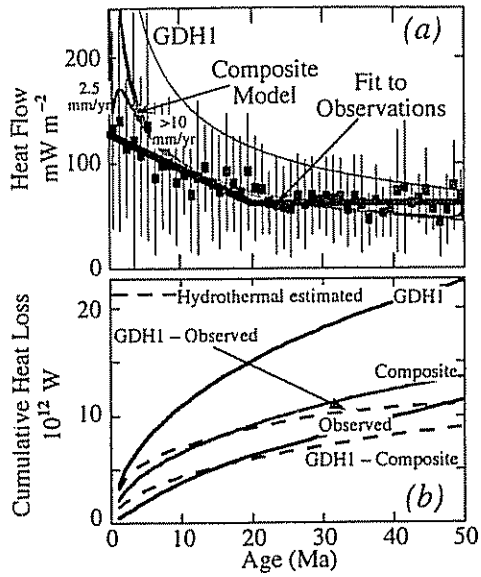

Figure 3. *a*: Observed oceanic heat flow means, standard deviations, and models with lithospheric age. Also shown are a simple two-stage linear fit to the data and the GDH1 model. The composite model prediction diverges at ages <5 Ma for half-spreading rates 2.5 and >10 mm/yr. *b*: Estimated cumulative hydrothermal heat losses inferred from differences between GDH1 and the observed heat loss (upper dashed line) and GDH1 and the composite model (lower dashed line). Also shown are cumulative heat loss curves for GDH1 and the composite model (upper curves) and the data (lower solid curve).

reflects the expected downward bias in the measurements which led us to use the seismicity and magma chamber depths instead as near-ridge constraints.

Hydrothermal Heat Flux

These results allow us to estimate the hydrothermal heat flux. The predicted heat flow (mW m^{-2}) for the GDH1 model, for ages t (Ma) < 50 Ma, is $q(t) = 510\, t^{-1/2}$. A numerical fit to the predicted heat flow for the composite model gives $q_c(t) = 308\, t^{-1/2}$. The crustal area for a given age is given approximately by $dA/dt = C_0\,(1 - t/180)$ where C_0 is the creation rate, 3.45×10^6 km^2 yr^{-1} [*Parsons*, 1981].

The cumulative predicted heat losses as a function of age (Figure 3b) for the GDH1 and composite models are

$$Q(t) = \int_0^t (dA/d\tau)\, q(\tau)\, d\tau \quad \text{and} \quad Q_c(t) = \int_0^t (dA/d\tau)\, q_c(\tau)\, d\tau,$$

so the cumulative hydrothermal heat loss predicted by the composite model is the difference, $Q_c^h(t) = Q(t) - Q_c(t)$. The mean observed heat flux is approximately $q_o(t) = 130 - 3.4t$ for $t \leq 20$ Ma and $q_o(t) = 62$ for $20 < t < 50$ Ma, so the cumulative observed heat loss $Q_o(t)$ and the corresponding cumulative inferred hydrothermal heat loss $Q_o^h(t)$ are simply computed.

Because $Q_c(t)$ exceeds $Q_o(t)$, the composite model predicts less cumulative hydrothermal heat loss than inferred from the data. By 50 Ma, $Q_c^h(t)$ is 9×10^{12} W, ~80% of the 11×10^{12} W inferred from the data. Most (85%) of the hydrothermal heat loss occurs for ages >1 Ma, and thus by off-axial and presumably low temperature water flow.

Figure 4a shows the predicted hydrothermal heat loss versus spreading rate for the axial region (defined as 0-0.1 Ma). Although model I was constrained by the seismicity and magma chamber depths to have deeper axial heat sinks, model II has more sinks integrated to 0.1 Ma and hence lower heat flow. Model I, for the slower rates, predicts ~1 W m^{-2} of hydrothermal heat loss, whereas model II, for faster rates, predicts about twice as much. More hydrothermal heat loss for rapid spreading seems plausible [*Baker and Hammond*, 1992], although direct data to confirm it is not available. Both estimates are smaller than the 3 W m^{-2} estimated from heat flow data alone [*Stein and Stein*, 1994], presumably due to the sampling bias.

The predicted hydrothermal heat flux per unit ridge length is useful for comparison with other estimates. At a slow ridge (10 mm/yr half-rate), the hydrothermal heat flux would be 1 W m^{-2} times the area on both sides of the axis within 0.1 Ma, or 2 MW per km ridge length. At 30 mm/yr half-rate (similar to the Juan de Fuca Ridge), hydrothermal heat flux within 0.1 Ma is 15 MW km^{-1}. This ~10 MW km^{-1} estimate for average spreading rates is similar to others [*Morton and Sleep*, 1985; *Stein and Stein*, 1994]. Comparison with field-based estimates is more difficult [*Dymond et al.*, 1988], because only a few areas have been studied, using various methods on different space and time scales. Estimates from seafloor vents along the Juan de Fuca Ridge are an order of magnitude lower, ~1 MW km^{-1} [*Bemis et al.*, 1993], perhaps because of missed vents and/or low temperature flow. Studies of hydrothermal plumes estimate their heat content at ~1000 MW [*Baker and Massoth*, 1987]. Assuming the plumes represent ~10 km ridge length, the estimated flux per unit ridge length is ~100 MW km^{-1}, an order of magnitude higher than our estimate. The discrepancy is not an artifact of the age interval sampled, as the plume studies

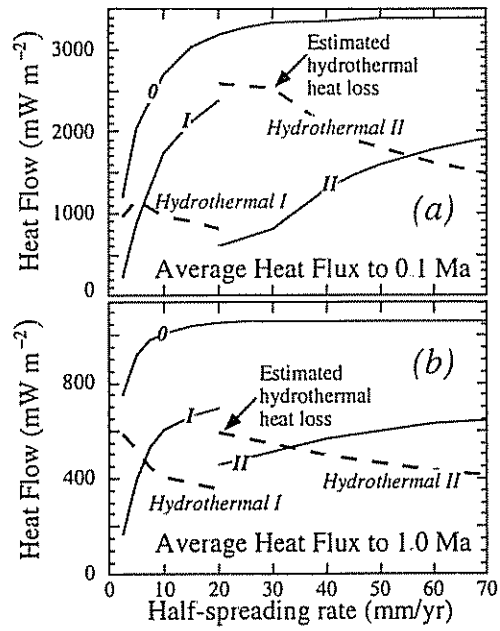

Figure 4. *a*: Average axial heat flux (to 0.1 Ma) for the composite model, assuming no hydrothermal circulation ("0") and for the two models. Dashed lines show predicted hydrothermal heat flux, the difference between "0" and the two models. The predicted hydrothermal heat loss is greater for fast spreading. *b*: Average near-axial heat fluxes (to 1.0 Ma). The predicted hydrothermal heat loss does not vary significantly with spreading rate.

extend a few km off-axis, comparable to the age interval we assume. Hence if both estimates are appropriate, observed plumes may be intermittent, in accord with the observation that only a fraction of the ridge (~20%) presently discharges plumes [*Baker and Hammond*, 1992]. Plumes also may sample water from further off-axis than 0.1 Ma. More data that sample larger areas of the ridge system over longer time periods will be needed to resolve these issues.

For greater distances from the axis, the model predictions depend less on spreading rate. The two models predict similar hydrothermal heat loss averaged over 0-1 Ma (Figure 4b), ~0.5 W m^{-2}. This is about half that inferred from the data, again presumably due to the sampling bias.

Discussion

Using seismicity and magma chamber constraints, we predict conductive heat flow for young lithosphere higher than observed, in accord with the idea that sampling biases the observations toward lower values. The results suggest that the bias is too small to dramatically change estimates of the net hydrothermal heat flux or the implication that most is off-axial. More sophisticated models of both the ridge axis and the hydrothermal flow can be made. However, we expect that although the predicted flux has uncertainties [*Stein and Stein*, 1994], and near-ridge measurements are scattered by local effects, our estimate of the fractional sampling bias is relatively robust. Our model assumptions about the equality of the near-ridge heat flow predict greater hydrothermal heat flux per unit ridge length along fast spreading ridges. This idea, though plausible, is not easily tested given the problems of heat flow site sampling and of reconciling the predicted time-averaged hydrothermal heat flux with the "instantaneous" estimates from plume and vent studies. These issues seem challenging and important for future research.

Acknowledgements. This research was supported by NSF grant EAR-9022476. We thank N. Sleep for helpful discussions.

References

Baker, E. T., and S. R. Hammond, Hydrothermal venting and the apparent magmatic budget of the Juan de Fuca Ridge, *J. Geophys. Res.*, *97*, 3443–3456, 1992.

Baker, E. T., and G. J. Massoth, Characteristics of hydrothermal plumes from two vent fields on the Juan de Fuca Ridge, *Earth Planet. Sci. Lett.*, *85*, 59–73, 1987.

Becker, K., and R. P. Von Herzen, Heat flow on western East Pacific Rise at 21°N, *J. Geophys. Res.*, *88*, 1057–1066, 1983.

Bemis, K. G., R. P. Von Herzen, and M. J. Mottl, Geothermal heat flux from hydrothermal plumes on the Juan de Fuca Ridge, *J. Geophys. Res.*, *98*, 6351–6365, 1993.

Davis, E. E., D. S. Chapman, C. B. Forster, and H. Villinger, Heat-flow variations correlated with buried basement topography on the Juan de Fuca Ridge, *Nature*, *342*, 533–537, 1989.

Dymond, J., E. Baker, and J. Lupton, Plumes: oceanic limb of seafloor hydrothermal systems, *The Mid-Ocean Ridge- A Global Dynamic System*, pp. 209–231, National Academy Press, Washington, D.C., 1988.

Fisher, A. T., K. Becker, T. N. Narasimhan, M. G. Langseth, and M. J. Mottl, Passive, off-axis convection through the Costa Rica Rift, *J. Geophys. Res.*, *95*, 9343–9370, 1990.

Huang, P. Y., and S. C. Solomon, Centroid depths of mid-ocean ridge earthquakes: dependence on spreading rate, *J. Geophys. Res.*, *93*, 13,445–13,477, 1988.

Langseth, M., K. Becker, R. P. Von Herzen, and P. Schultheiss, Heat and fluid flux through sediment on the flank of the mid-Atlantic ridge, *Geophys. Res. Lett.*, *19*, 517–520, 1992.

Lin, J., and E. M. Parmentier, Mechanisms of lithospheric extension at mid-ocean ridges, *Geophys. J.*, *96*, 1–22, 1989.

Lowell, R., Topographically driven hydrothermal convection in oceanic crust, *Earth Planet. Sci. Lett.*, *49*, 21–28, 1980.

Morton, J. L., and N. H. Sleep, A mid-ocean ridge thermal model: Constraints on the volume of axial hydrothermal heat flux, *J. Geophys. Res.*, *90*, 11,345–11,353, 1985

Parsons, B., The rates of plate creation and consumption, *Geophys. J. R. astron. Soc.*, *67*, 437–448, 1981.

Phipps Morgan, J., and Y. J. Chen, The genesis of oceanic crust: Magma injection, hydrothermal circulation, and crustal flow, *J. Geophys. Res.*, *98*, 6283–6297, 1993.

Purdy, G. M., L. S. L. Kong, G. L. Christeson, and S. C. Solomon, Relationship between spreading rate and the seismic structure of mid-ocean ridges, *Nature*, *355*, 815–817, 1992.

Rona, P. A., K. Bostrom, L. Laubier, and K. L. Smith, *Hydrothermal Processes at Seafloor Spreading Centers*, 796 pp., Plenum, New York, 1983.

Sleep, N. H., and T. J. Wolery, Egress of hot water from the midocean ridge hydrothermal systems: some thermal constraints, *J. Geophys. Res.*, *83*, 5913–5922, 1978.

Stein, C. A., and S. Stein, A model for the global variation in oceanic depth and heat flow with lithospheric age, *Nature*, *359*, 123–129, 1992.

Stein, C. A., and S. Stein, Constraints on hydrothermal heat flux through the oceanic lithosphere from global heat flow, *J. Geophys. Res.*, *89*, 3081-3095, 1994.

Toomey, D. R., S. C. Solomon, and G. M. Purdy, Microearthquakes beneath the median valley of the Mid-Atlantic Ridge near 23°N: Tomography and tectonics, *J. Geophys. Res.*, *93*, 9093–9112, 1988.

Wiens, D. A., and S. Stein, Age dependence of oceanic intraplate seismicity and implications for lithospheric evolution, *J. Geophys. Res.*, *88*, 6455–6468, 1983.

A. M. Pelayo and S. Stein, Department of Geological Sciences, Northwestern University, Evanston, IL 60208-2150.

C. A. Stein, Geological Sciences, m/c 186, University of Illinois at Chicago, 845 W. Taylor St., Chicago, IL 60607-7059.

(Received Sept. 20, 1993; revised Jan. 26, 1994;
accepted Jan. 30, 1994.)